Journal of Thermal Science Vol.28, No.5 (2019) 1065−1077

https://doi.org/10.1007/s11630-019-1127-3 **Article ID: 1003-2169(2019)05-1065-13**

Study on the Performance of Organic Rankine Cycle-Heat Pump (ORC-HP) Combined System Powered by Diesel Engine Exhaust

ZHAO Tenglong[1,2], YU Fei[1,2], ZHANG Hongguang[1,2,*], WU Yuting[1,2], WANG Yan[1,2]

1. College of Environmental and Energy Engineering, Beijing University of Technology, Beijing 100124, China
2. MOE (Ministry of Education) Key Laboratory of Enhanced Heat Transfer and Energy Conservation, Beijing Key Laboratory of Heat Transfer and Energy Conversion, Beijing University of Technology, Beijing 100124, China

Abstract: This study presents an ORC-HP combined system driven by diesel engine exhaust. This paper focuses on the feasibility and performance of the combined system under heating mode to heat a coach. The performances of the combined system with different parameters, including condensation temperature and evaporation pressure in ORC system, gas cooler outlet pressure, gas cooler outlet temperature and evaporation temperature in HP system, have been analyzed. The results show that the combined system can fully meet the demand of heat production. The optimal flow division ratio (r_p) of 0.32 is selected by analyzing the system performance. Low condensation temperature is beneficial to the combined system performance. There exists a suitable range of evaporation temperature, gas cooler outlet pressure and gas cooler outlet temperature to achieve excellent performance. The heating coefficient of performance (COP_h) shows a first increasing and then decreasing trend with gas cooler outlet pressure, namely there exists an optimal gas cooler outlet pressure that achieves the maximum COP_h. The maximum total efficiency, COP_h and heating capacity can reach up to 48.44%, 4.78 and 176.56 kW, respectively. These results show significant energy savings by applying the ORC-HP combined system.

Keywords: organic Rankine cycle, heat pump, combined system, total efficiency, COP_h

1. Introduction

With global energy usage continuing to rise, many research institutes and universities are demonstrating a commitment to energy saving both domestically and across the globe. For China, the number of car ownership is more than 200 million by 2017. However, the effective efficiency from internal combustion engine (ICE) is approximately 25% to 45%, and the remaining energy is wasted in cooling, exhaust, and mechanical losses. Thus, improving the efficiency of ICE has become the hot research topics [1-3].

ORC technology is deemed to be a promising method to convert low-grade waste heat into useful work in engine waste heat recovery [4, 5]. Song et al. used ORC system to recover the compressed natural gas engine. The results showed that the thermal efficiency of 5% could be acquired [6]. Yang et al. designed a dual loop ORC system to take advantage of the diesel engine waste heat. The results revealed that the largest net power output could reach 27.85 kW under the rated condition [7-8]. Zhao et al. stated that a maximum net power output of

Received: Dec 26, 2018
AE: MANENTE Giovanni
Corresponding author: ZHANG Hongguang E-mail: zhanghongguang@bjut.edu.cn

Nomenclature

c_p	the constant pressure specific heat capacity/kJ·kg^{-1}·K^{-1}	ehe	exterior heat exchanger
Ex	exergy destruction rate/kW	evap	evaporator
ex	specific exergy/kJ·kg^{-1}	exh	exhaust
h	enthalpy/kJ·kg^{-1}	exp	expander
m	mass flow rate/kg·s^{-1}	f	working fluid
P	net power output/kW	h	heating
p	pressure/MPa	ihe	interior heat exchanger
Q	heat transfer rate/kW	mech	mechanical
r_p	flow division ratio	p	pump
s	entropy/kJ·kg^{-1}·K^{-1}	re	recuperator
T	temperature/K	s	isentropic process
W	rate of work or power/kW	sh	shaft
Greek letters		t	total
ε	effectiveness of recuperator	v	expansion valve
η	efficiency	**Acronyms**	
Subscript		CCHP	combined cooling, heating and power
0	dead (reference) state	CHP	combined heat and power
1, 2, 2s …	state point in ORC system	*COP*	coefficient of performance
1', 2', 3'…	state point in HP system	FEL	following the electric load
I, II, III, IV	state point inside temperature of the coach	FTL	following the thermal load
C	CO_2	HP	heat pump
comp	compressor	ICE	internal combustion engine
con	condenser	ORC	organic Rankine cycle
e	power generation		

4.13 kW and the thermal efficiency increment of 0.66 % were acquired [9]. Yu et al. presented an ORC-ICE simulation model and the findings indicated that the recovery efficiency of 9.2% could be obtained under the rated condition [10]. Song et al. investigated an optimized ORC system simulation model about marine diesel engines, and the conclusions indicated that the system was economically attractive [11,12].

Besides, working fluids have a significant effect on the performances of the ORC system. Several working fluids were selected in Refs. [13, 14] and used in waste heat recovery. Tian et al. estimated multifarious working fluids to recover the ICE exhaust heat in an ORC system. The results presented the highest thermal efficiency of R141b, R245fa and R152a ranging from 16.60% to 11.80%, and expressed the lowest electricity production cost values ranging from 0.30 to 0.384 $/kWh [15]. Wang et al. took different pure working fluids into consideration to assess the performances of the ORC system. The results indicated that R245fa was eco-friendly working fluids for ORC to recover the exhaust gas waste heat. [16]. Feng et al. analyzed the waste heat utilization using R123, R245fa and their mixtures and found that R245fa had a better net electricity output [17]. Hence, R245fa is adopted as the working fluid of the ORC system in this study.

Heating and cooling thermally driven by vapor compression cycle had a promising future due to its high coefficient of performance (*COP*) basing on the Ref. [18]. The performances of combined heat and power (CHP) and combined cooling, heating and power (CCHP) systems operating following the thermal load (FTL) and following the electric load (FEL) were presented by Mago et al. They revealed that both systems operating FTL lessened the electricity consumption for all the discussed cities [19]. Li et al. proposed a transcritical CO_2 HP system driven by CO_2 Rankine cycle, and they found that the whole system cooling *COP* and heating *COP* can be above 0.3 and 0.9, respectively [20]. To solve the influence of the ratio between electricity and thermal energy output on the performances of CCHP system, Fang et al. proposed a CCHP-ORC system, which could adjust the ratio by altering the loads of ORC and electric chiller, and the results showed that the

performances of CCHP-ORC system were better than conventional CCHP system [21]. Agrawal et al. developed a CO_2 heat pump system using capillary tube to act as an expansion valve for water cooling and heating [22]. Antonijevic et al. tested a heat pump supplemental heating system in vehicle at low temperature working conditions, and the performance, fuel consumption and operational behavior were superior to other heating solutions [23]. Wang et al. explored the heating performances of prototype heat pump system for automotive under low ambient temperature working conditions, and the results showed that the system performances had the potential for improvement [24,25]. And the same conclusions could be seen in Refs. [26,27] where the heat pump was applied to the electric vehicles. Therefore, CO_2 is employed as the working fluid of HP system in this study.

Today, coaches are still in great use. The researches on combined cooling, heating and power with the actual operation conditions of diesel engine need to be further explored. A detailed performance analysis is conducted based on thermodynamic analysis and several indicators such as total efficiency, heating capacity, net power output and total exergy destruction is estimated. This paper will provide a key guidance on the application of an actual ORC-HP system that is suitable for engine waste heat recovery.

2. ORC-HP Combined System Description

This paper proposes an ORC-HP combined system (combined system), which is composed of an ORC system and a transcritical CO_2 HP system. The purpose of the combined system is to generate electricity and adjust the inside temperature of the coach. Fig. 1 shows the illustrative diagram of the combined system. The expander of ORC system and compressor of the HP system are connected by a drive shaft. The clutch in the middle of the drive shaft can transfer or cut off the torque transmission between the expander and compressor.

The ORC system with recuperator, which mainly consists of an evaporator, a turbine expander, a condenser, a reservoir, a pump and a recuperator used to enhance the energy conversion efficiency effectively. The low-pressure, saturated liquid R245fa (Fig. 1, state 1) is pressurized by the pump (Fig. 1, state 2) and then is preheated in the recuperator (Fig. 1, state 3). Subsequently, the R245fa absorbs heat from evaporator and reaches its superheated and high-temperature state (Fig. 1, state 4). The superheated R245fa vapor enters expander to rotate the drive shaft, which further drives the compressor and generator, simultaneously. R245fa vapor expelled from expander (Fig. 1, state 5) is cooled in the recuperator (Fig. 1, state 6) and then flows into the condenser and reservoir. The corresponding *T-s* diagram of the ORC system is demonstrated in Fig. 2(a).

The HP system mainly includes a compressor, a four-way reversing valve, an expansion valve, an interior heat exchanger and an exterior heat exchanger. In the HP system, the subcritical CO_2 (Fig. 1, state 1') is compressed to supercritical state (Fig. 1, state 2') by compressor which is powered by turbine of the ORC system. Subsequently, CO_2 flows into heat exchanger through the four-way reversing valve. The specific path of the CO_2 flow depends on the operation mode of the HP system, and the details are as follows. The corresponding *T-s* diagram of the HP system is demonstrated in Fig. 2(b).

2.1. Operation mode

The diesel engine exhaust is divided into two parts by valve 2 under heating mode. The flow division ratio r_p is defined as the ratio of the exhaust mass flow rate in HP system to the diesel engine exhaust mass flow rate. One part of exhaust (r_p) is used to preheat the exterior heat exchanger of the HP system. The exhaust temperature is much higher than ambient temperature, thus the frosting problem of exterior heat exchanger can be solved by this way even at the extremely low ambient temperature. The other part of exhaust ($1-r_p$) is used as the heat source to ORC system.

The exterior heat exchanger is used as an evaporator to absorb exhaust heat under heating mode. CO_2 reaches to high-temperature state (Fig. 1, state 6') after heated by exterior heat exchanger. Then CO_2 enters the compressor through the four-way reversing valve from port B to port C. Subsequently, supercritical CO_2 flows into the interior heat exchanger to heat the coach through the four-way reversing valve from port D to port A. CO_2 flows into the exterior heat exchanger through the expansion valve, and finally the whole heating mode is completed.

The temperature T_I and T_{II} ($T_I < T_{II}$) are set in the coach in advance, and the inside temperature of the coach is monitored by temperature sensor. When the inside temperature of the coach is lower than T_I, the valve 3 is opened, then the clutch is in a state of connection and the interior heat exchanger of the HP system heats the coach. When the inside temperature of the coach reaches T_{II}, the clutch is cut off and the valve 3 is closed, then all the exhaust is supplied to the ORC system through valve 2 and valve 1. When the temperature is lower than T_I, the clutch is connected and the HP system will work again. In this way, the intermittent work of the HP system ensures that the inside temperature of the coach fluctuates within a reasonable range.

The valve 3 closes completely under cooling mode, and all of exhaust flows into the ORC system to generate

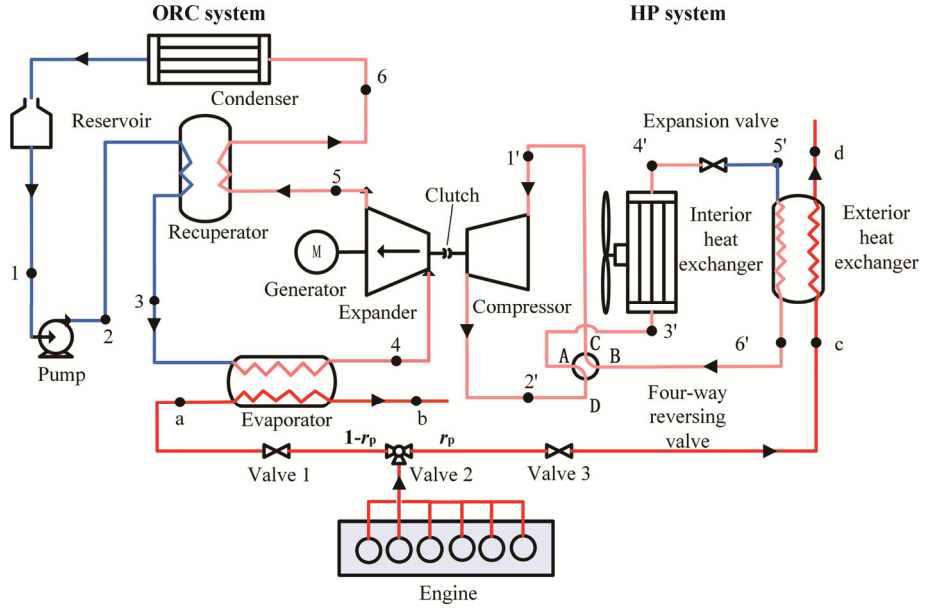

Fig. 1 Schematic diagram of the ORC-HP combined system

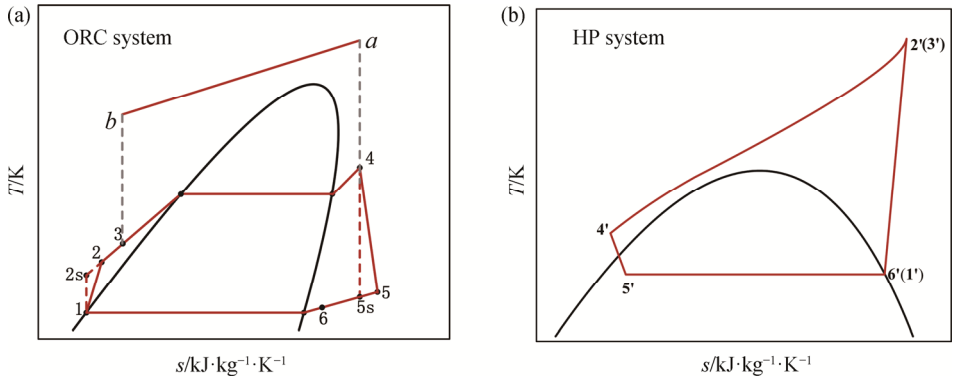

Fig. 2 *T-s* diagram of the ORC system and HP system under heating mode

power. The compressor of the HP system is driven by drive shaft or purely powered by electricity when the expander cannot provide sufficient power. The other difference with heating mode is the flow path of the CO_2 through four-way reversing valve. The compressed CO_2 flows into exterior heat exchanger to release heat through four-way reversing valve from port D to port B. There is an expansion valve between interior and exterior heat exchanger. After the CO_2 cooled in exterior heat exchanger flows through the expansion valve, it flows into the interior heat exchanger to cool the coach. The interior heat exchanger and inlet port of compressor are connected by the four-way reversing valve from port A to port C. In this way, the HP system can achieve the refrigeration function, and the cycle recommences.

The temperature T_{III} and T_{IV} (T_{III}< T_{IV}) are set in the coach in advance. When the inside temperature of the coach is higher than T_{IV}, the HP system is under operation state; when the inside temperature reaches T_{III}, the clutch is disconnected and the HP system stops working.

When the vehicle temperature is higher than T_{IV}, the HP system will work again. In this way, the intermittent work of the HP system ensures that the inside temperature of the coach changes within a reasonable range.

2.2. Parameters of diesel engine

The exhaust energy changes with the operation conditions of the WP10.336NCB diesel engine. A six-cylinder in-line diesel engine is acted as the heat source of the combined system. The amount of available heat in the exhaust depends on the engine operation conditions, which have an essential impact on the operation performance of the ORC-HP combined system. Accordingly, it is significant to research the characteristics of the exhaust energy under different operation conditions. The main characteristics of the WP10.336NCB diesel engine are listed in Table 1.

Table 1 WP10.336NCB diesel engine main characteristics

Item	Parameters	Unit
Rated power	280	kW
Maximum torque	1500	N·m
Displaced volume	9.726	L
Bore	126	mm
Rated speed	2200	r/min
Stroke	130	mm
Compression ratio	17:1	-

The exhaust temperature of the diesel engine under various operating conditions is shown in Fig. 3(a). The engine exhaust temperature increases with engine torque. The reason for this is that: when engine speed is constant, the increase of the engine torque is depended on increasing fuel injection which can increase the temperature of mixture gas after combustion, so the exhaust temperature increases. It can be calculated that the maximum exhaust temperature is about 818.5 K. Moreover, the maximum exhaust energy rate can reach 280 kW when engine exhaust temperature and speed are 818 K and 2200 r/min, respectively. The variation of engine exhaust mass flow rate with the engine speed and torque is shown in Fig. 3(b). As the engine speed and torque increase, exhaust mass flow rate increases. When the engine speed is 2200 r/min and the engine torque is 1215 N·m, the exhaust mass flow rate reaches a maximum value of 0.48 kg/s.

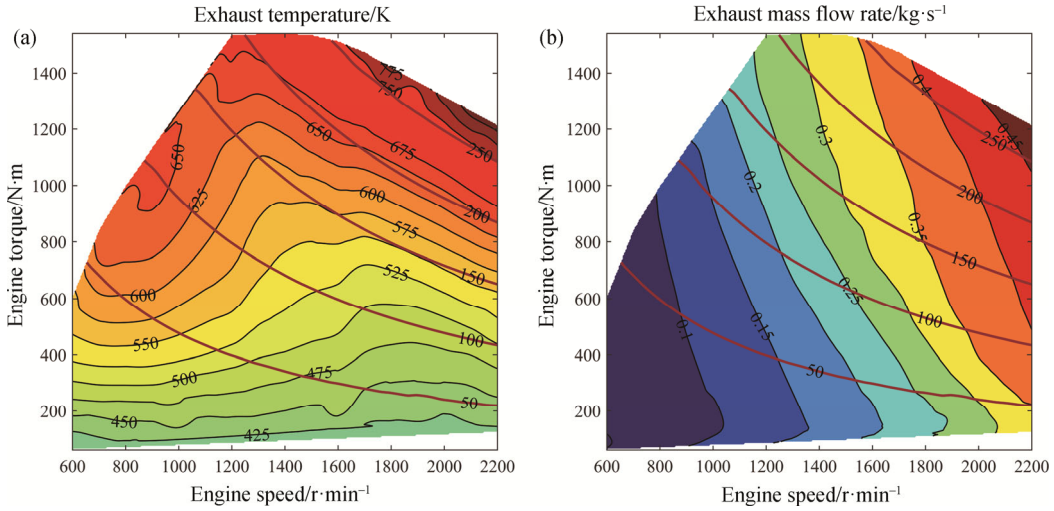

Fig. 3 Variation of the exhaust temperature, available exhaust energy rate (represented by the various red curves in kW) and exhaust mass flow rate with the engine speed and torque

3. Thermodynamic Analysis of the ORC-HP Combined System

The thermodynamic model for the combined system is employed based on the first and second laws of thermodynamics. Steady flow energy equations in view of the energy balance and exergy balance for components of the system are employed in each case. Some assumptions under heating mode have been made for ORC-HP combined system as follows:

(1) Heat transfer between the coach and ambient is negligible;

(2) The compression process is adiabatic but non-isentropic;

(3) The evaporation and vapor cooling processes are isobaric;

(4) The pressure loss and heat rejection to the environment of the recuperator are not considered. The recuperator effectiveness of 80% is adopted [28];

(5) The power generation efficiency, expander isentropic efficiency and pump isentropic efficiency are set to 90%, 85% and 85%, respectively [29];

(6) Rated heating capacity is set to 15 kW [30].

The relative influence factors of ORC-HP combined system are shown in Table 2.

Table 2 Range of variable parameters

Variable parameters	Range	Unit
Condensation temperature in ORC system (T_1)	303–323	K
Evaporation pressure in ORC system (p_4)	1–3	MPa
Gas cooler outlet pressure in HP system ($p_{4'}$) [31]	8–13	MPa
Gas cooler outlet temperature in HP system ($T_{4'}$)	303–323	K
Evaporation temperature in HP system ($T_{6'}$)	273–287	K

The maximum available exhaust energy rate for ORC-HP combined system is given by:

$$Q_{\mathrm{exh}} = c_{\mathrm{p}} m_{\mathrm{exh}} \left(T_{\mathrm{exh}} - T_{\mathrm{min}}\right) \tag{1}$$

where m_{exh} is the exhaust mass flow rate; T_{exh} is the exhaust temperature at the points a and c in Fig. 1; T_{min} is exhaust temperature at the outlet of the evaporator (points b and d). Considering the corrosion for metal heat exchanger, the temperature of flue gas is scarcely allowed to drop below the sulfur trioxide dew point during heat exchange process [32]. Therefore, the exhaust temperature at the outlet of evaporator is specified as 388.15 K.

c_{p} is the constant pressure specific heat capacity of the exhaust:

$$c_{\mathrm{p}} = 0.00025 \times T_{\mathrm{exh}} + 0.99 \tag{2}$$

According to the energy conservation law, the heat transfer rate of exhaust is equal to the heat absorption of the working fluid:

$$Q_{\mathrm{evap}} = Q_{\mathrm{exh}} \times \left(1 - r_{\mathrm{p}}\right) \tag{3}$$

Q_{exh} is the total energy rate of the diesel engine exhaust.

The heat transfer rate and exergy destruction rate of the evaporator are determined as:

$$Q_{\mathrm{evap}} = m_{\mathrm{f}} \left(h_4 - h_3\right) \tag{4}$$

$$Ex_{\mathrm{evap}} = T_0 m_{\mathrm{f}} \left[\left(s_4 - s_3\right) - \frac{h_4 - h_3}{T_{\mathrm{exh}}} \right] \tag{5}$$

The output work and exergy destruction rate of the expander are determined as:

$$W_{\mathrm{exp}} = m_{\mathrm{f}} \left(h_4 - h_5\right) \tag{6}$$

$$Ex_{\mathrm{exp}} = m_{\mathrm{f}} \left(ex_4 - ex_5\right) - W_{\mathrm{exp}} \tag{7}$$

W_{sh} is the shaft work of the ORC system and can be described as:

$$W_{\mathrm{sh}} = W_{\mathrm{exp}} \eta_{\mathrm{mech}} \eta_{\mathrm{sh}} \tag{8}$$

where η_{mech} is the mechanical efficiency of the expander, which is assumed to be 90%; η_{sh} is the transmission efficiency of the shaft, which is assumed to be 90% [33].

The heat transfer rate and exergy destruction rate of the condenser are denoted as:

$$Q_{\mathrm{con}} = m_{\mathrm{f}} \left(h_6 - h_1\right) \tag{9}$$

$$Ex_{\mathrm{con}} = m_{\mathrm{f}} \left[h_6 - h_1 - T_0 \left(s_6 - s_1\right) \right] \tag{10}$$

The power consumed and exergy destruction rate of the pump are calculated as:

$$W_{\mathrm{p}} = m_{\mathrm{f}} \left(h_2 - h_1\right) \tag{11}$$

$$Ex_{\mathrm{p}} = T_0 m_{\mathrm{f}} \left(s_2 - s_1\right) \tag{12}$$

The energy equation and the exergy destruction rate of the recuperator are given:

$$h_3 - h_2 = h_5 - h_6 \tag{13}$$

$$Ex_{\mathrm{re}} = T_0 m_{\mathrm{f}} \left(s_3 - s_2 + s_6 - s_5\right) \tag{14}$$

$\varepsilon_{\mathrm{re}}$ is the regenerative efficiency of the recuperator, which can be calculated as follow:

$$\varepsilon_{\mathrm{re}} = \frac{T_5 - T_6}{T_5 - T_2} \tag{15}$$

For HP system, some equations are represented as follows:

For compressor:

$$W_{\mathrm{comp}} = W_{\mathrm{sh}} \tag{16}$$

$$W_{\mathrm{comp}} = m_{\mathrm{C}} \left(h_{2'} - h_{1'}\right) \tag{17}$$

$$Ex_{\mathrm{comp}} = W_{\mathrm{comp}} + m_{\mathrm{C}} \left(ex_{1'} - ex_{2'}\right) \tag{18}$$

The adiabatic efficiency of the compressor is presented as [31]:

$$\eta_{\mathrm{comp}} = 1.0003 - 0.121 \frac{p_{2'}}{p_{1'}} \tag{19}$$

For exterior heat exchanger:

$$Q_{\mathrm{ehe}} = m_{\mathrm{C}} (h_{6'} - h_{5'}) \tag{20}$$

For expansion valve:

$$h_{4'} = h_{5'} \tag{21}$$

$$Ex_{\mathrm{v}} = m_{\mathrm{C}} \left(ex_{5'} - ex_{4'}\right) \tag{22}$$

For interior heat exchanger:

$$Q_{\mathrm{ihe}} = m_{\mathrm{C}} \left(h_{4'} - h_{3'}\right) \tag{23}$$

$$Ex_{\mathrm{ihe}} = m_{\mathrm{C}} \left(ex_{4'} - ex_{3'}\right) + Q_{\mathrm{ihe}} \left(1 - \frac{T_0}{T_{\mathrm{h}}}\right) \tag{24}$$

where T_0 is atmospheric temperature; T_{h} is logarithmic mean temperature difference of interior heat exchanger.

The total exergy destruction rate of ORC system is written as:

$$Ex_{\mathrm{ORC}} = Ex_{\mathrm{evap}} + Ex_{\mathrm{exp}} + Ex_{\mathrm{re}} + Ex_{\mathrm{con}} + Ex_{\mathrm{p}} \tag{25}$$

The total exergy destruction rate of the HP system is determined as:

$$Ex_{\mathrm{HP}} = Ex_{\mathrm{comp}} + Ex_{\mathrm{ihe}} + Ex_{\mathrm{ehe}} + Ex_{\mathrm{v}} \tag{26}$$

The total exergy destruction rate of the ORC-HP combined system is the sum of ORC system and HP system:

$$Ex_{\mathrm{total}} = Ex_{\mathrm{ORC}} + Ex_{\mathrm{HP}} \tag{27}$$

The performance of the ORC-HP combined system is evaluated by heating coefficient of performance (COP_{h}) and total efficiency. The COP_{h} is the ratio of heating capacity in HP system to the power consumption of the compressor in the HP system. It is calculated as:

$$COP_{\mathrm{h}} = \frac{Q_{\mathrm{ihe}}}{W_{\mathrm{comp}}} \tag{28}$$

The net power output generated by the combined system is described as:

$$P = \left(W_{\mathrm{exp}} - W_{\mathrm{com}}\right) \eta_{\mathrm{e}} - W_{\mathrm{p}} \tag{29}$$

The total efficiency of the combined system is presented as:

$$\eta_{\mathrm{t}} = \frac{Q_{\mathrm{ihe}} + P}{Q_{\mathrm{exh}}} \tag{30}$$

4. Results and Discussion

By way of recovering diesel engine exhaust energy as much as possible, it is needed to identify some boundary conditions to explore the effect of different parameters on the performance of the combined system.

The condensation temperature in ORC system is 313 K, evaporation pressure in ORC system is 3 MPa, gas cooler outlet pressure in HP system is 10 MPa, gas cooler outlet temperature in HP system is 313 K, evaporation temperature in HP system is 283 K, ambient temperature is 273 K and the degree of superheating of R245fa is 10 K. All the above conditions are defined as the reference operation condition. The control variable method is used to analyze the impact of these parameters on the combined system performance.

The variation of r_p has a great impact on net power output of combined system, which can be drawn from following figures. The HP system is purely driven by drive shaft when r_p is 0, and the maximum amount of power available is 29.60 kW. The net power generated by the combined system cannot meet the needs of required heating capacity under the operation conditions when exhaust temperature and engine speed are low.

The net power gradually decreases to 0 with increasing r_p. The critical value of the net power output of the combined system can be obtained when r_p is 0.32. Specially, the reason for the negative value in Fig. 4 is

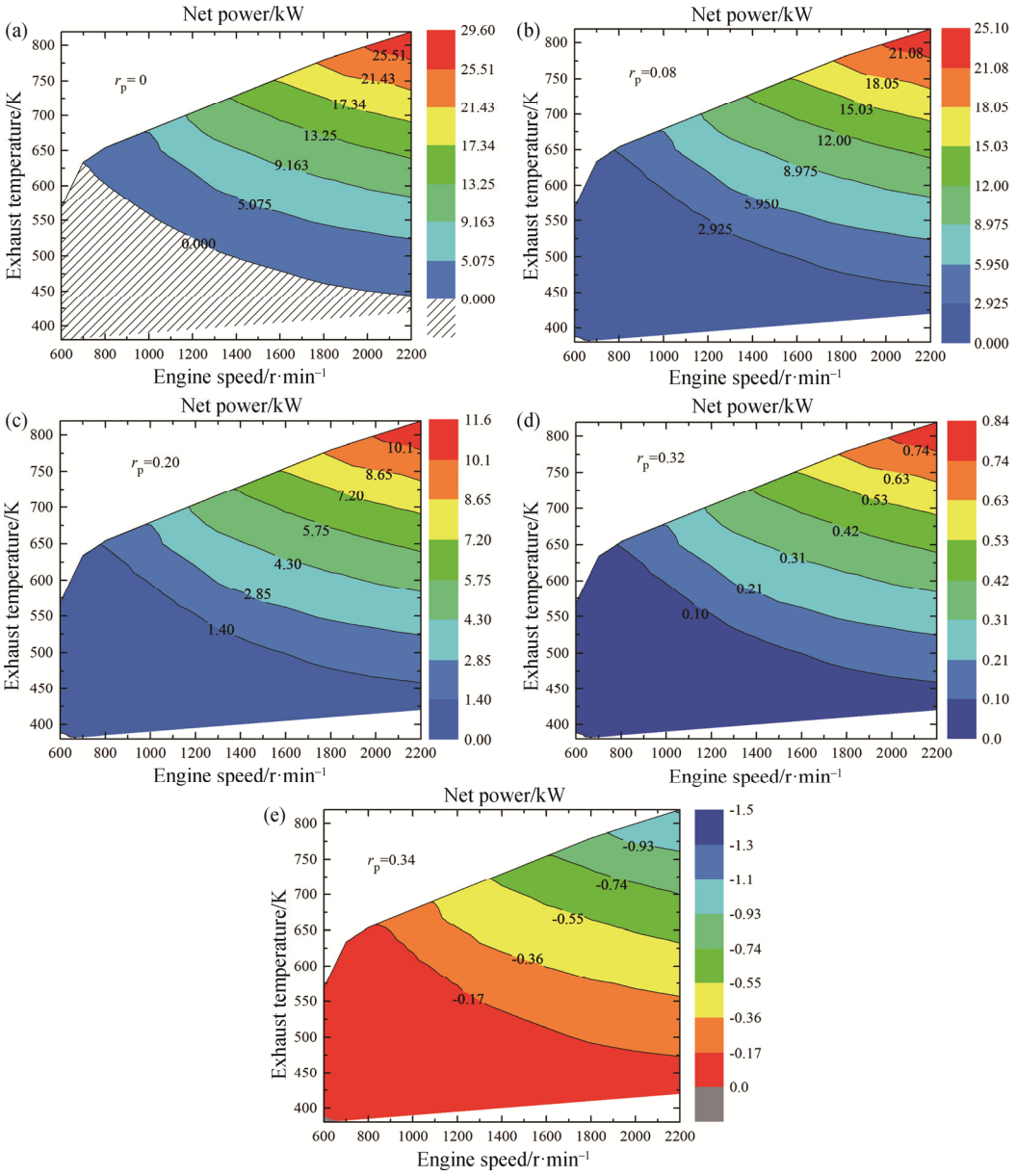

Fig. 4 The net power output of ORC-HP combined system with the engine speed and T_{exh} under different r_p

that the heating capacity of the HP system cannot meet the value of rated heating capacity (15 kW). When r_p is equal to 0.08, 0.20 and 0.32, the net power output is calculated by Eq. (29), and it decreases gradually with the rise of r_p and decrease of engine speed.

Available power is the sum of net power output and heating capacity in ORC and HP system. Fig. 5 illustrates the maximum available power variation with the exhaust temperature under different r_p. The results show that available power rises with the exhaust temperature. Moreover, in general, when the exhaust temperature is higher than 475 K, the higher r_p is, the more available power can be gained.

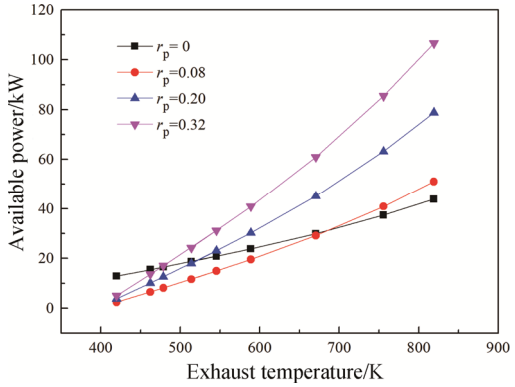

Fig. 5 The maximum available exhaust energy rate with T_{exh} under different r_p

Fig. 6 shows the change of net power output and total exergy destruction of the combined system. Net power output of the combined system lessens obviously with increasing condensation temperature of ORC. Compared with the reference operation conditions, low condensation temperature is conducive to improving the performance of the combined system. In addition, the maximum net power output increases by 3.0 kW on the basis of reference operation conditions. When the condensation temperature rises to 323 K, the negative value of the net power output can be obtained, which indicates that the power consumption by compressor is more than the power generated by expander under these operation conditions. Additionally, the total exergy destruction of the ORC-HP combined system increases with increasing exhaust temperature and engine speed, such as shown in Fig. 6(b). Moreover, condensation temperature has a slight influence on the total exergy destruction.

Fig. 7(a) exhibits the exergy destruction variation in ORC system with evaporation pressure. The exergy destruction of evaporator and condenser decreases with increasing evaporation pressure, and most of the exergy destruction is in evaporator and condenser, whereas the exergy destruction in pump is the lowest, which is close to 0. When evaporation pressure rises from 1.0 MPa to 3.0 MPa, the exergy destruction in evaporator decreases from 71.90 kW to 60.81 kW, and that of expander increases from 2.65 kW to 4.20 kW. Therefore, the total exergy destruction decreases from 94.11 kW to 83.70 kW for ORC system. Moreover, Fig. 7(b) shows that the total exergy destruction of the combined system decreases slightly with increasing evaporation pressure. When exhaust temperature and engine speed are 818 K and 2200 r/min, respectively, the total exergy destruction decreases from 161.90 to 151.56 kW. It varies rapidly with the exhaust temperature and engine speed. Similarly, the higher the engine speed and exhaust temperature are, the higher total exergy destruction is.

Fig. 8 shows the varying trend of total efficiency and COP_h with gas cooler outlet pressure of HP system. The total efficiency shows a first rapidly decreasing and then slowly increasing trend with gas cooler outlet pressure of HP system. Furthermore, the total efficiency decreases from 48.44% to 42.96% when the gas cooler outlet pressure HP varies from 8 MPa to 9.5 MPa. In addition,

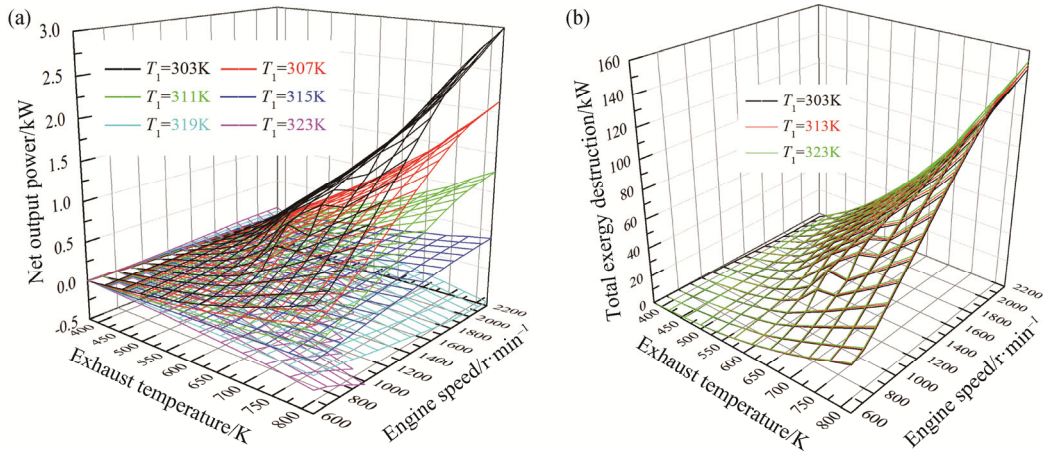

Fig. 6 Net power output and total exergy destruction with condensation temperature of ORC system

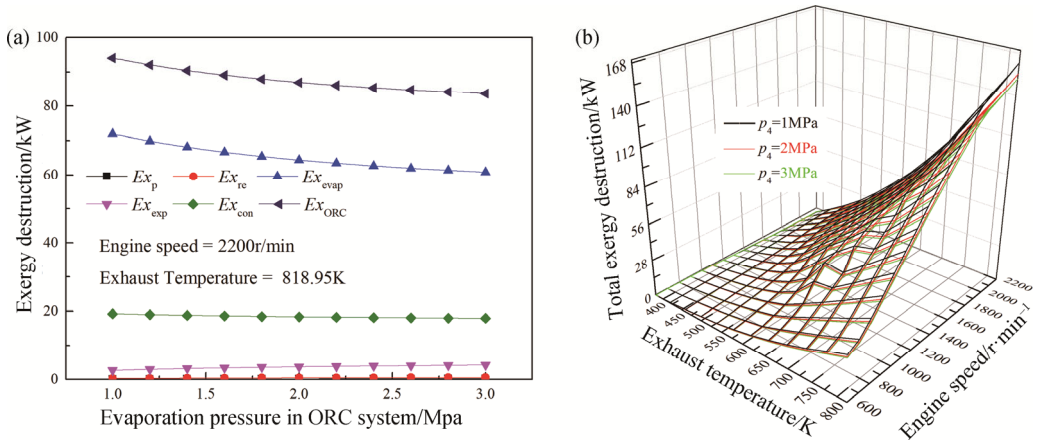

Fig. 7 Exergy destruction with evaporation pressure of ORC system

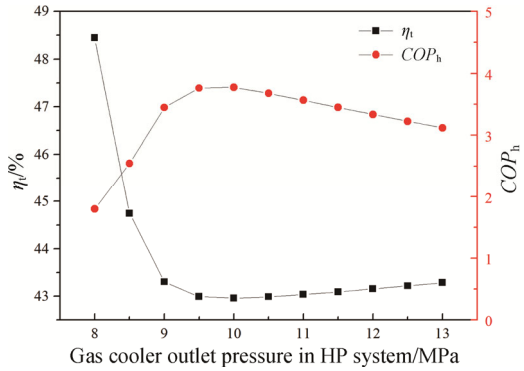

Fig. 8 Total efficiency and COP_h with gas cooler outlet pressure of HP system

the total efficiency only increases from 42.96% to 43.81% when the gas cooler outlet pressure rises from 9.5 MPa to 13 MPa.

Contrary to the curve of the total efficiency, the COP_h shows a first increasing and then decreasing trend with the gas cooler outlet pressure, namely there exists an optimal gas cooler outlet pressure that achieves the maximum COP_h. The COP_h increases rapidly from 1.79 to 3.76 when the gas cooler outlet pressure varies from 8 to 10 MPa, and the peak value of 3.76 is obtained when the gas cooler outlet pressure is 10 MPa, then the COP_h decreases slightly to 3.12 with the increment of gas cooler outlet pressure.

Fig. 9(a) shows the net power output variation with gas cooler outlet pressure. Generally, the net power output goes up at first and then decreases with the gas cooler outlet pressure. The higher the exhaust temperature is, the more obvious the change of net power output is. Moreover, when the gas cooler outlet pressure rises from 9.5 MPa to 11 MPa, the higher the exhaust temperature is, the higher the net power output is, and the value of it is higher than 0, namely the power from expander is enough to drive the HP system. When gas cooler outlet

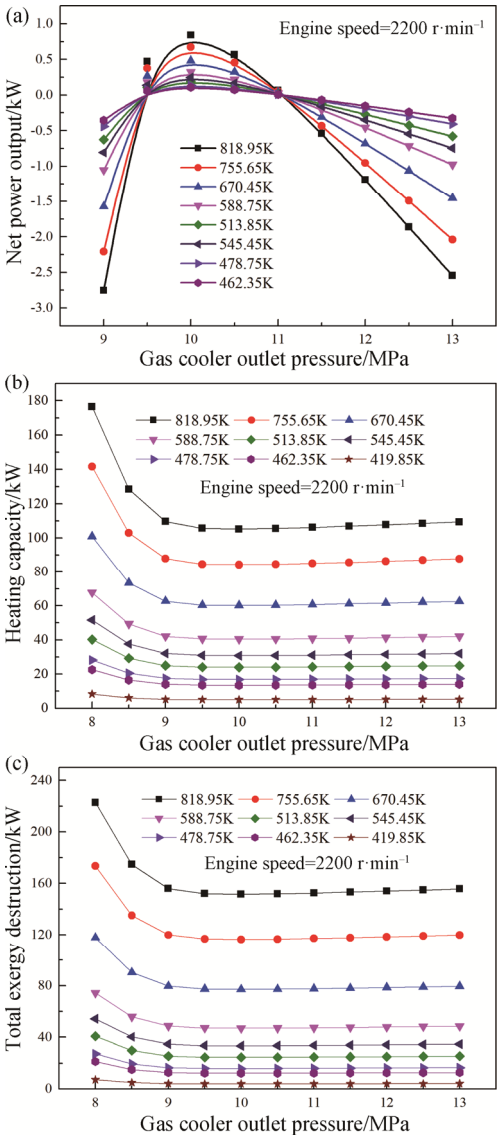

Fig. 9 Net power output, heating capacity and total exergy destruction with gas cooler outlet pressure of HP system

pressure is less than 9.5 MPa and more than 11 MPa, the value of it is negative. The higher the exhaust temperature is, the lower the net power output is. Therefore, there exists a suitable operation range of the gas cooler outlet pressure for the combined system.

Fig. 9(b) and Fig. 9(c) show the variation of heating capacity and total exergy destruction with gas cooler outlet pressure. It is interesting that the variation of heating capacity and total exergy destruction is similar: it first decrease rapidly and then tend to stabilize with the gas cooler outlet pressure. Additionally, the higher the exhaust temperature is, the greater the heating capacity is. Fig. 9(b) shows that the maximum heating capacity of the HP system decreases first from 176.56 to 105.27 kW, and then increases to 109.41 kW with the variation of gas cooler outlet pressure. When the gas cooler outlet pressure varies from 8 to 10 MPa, the maximum heating capacity rapidly reduces and reaches the valley value of 105.27 kW under the reference operation conditions. Subsequently, the heating capacity changes from 105.27 to 109.41 kW with the gas cooler outlet pressure.

Fig. 10 shows the varying trend of total efficiency and COP_h under different gas cooler outlet temperature of HP system. Similar to the effect of gas cooler outlet pressure on the performance of combined system, the total efficiency and COP_h have a contrary tendency with gas cooler outlet temperature. As shown in Fig. 10, the total efficiency increases from 42.54% to 47.06% with gas cooler outlet temperature, and the higher of the gas cooler outlet temperature is, the faster total efficiency grows. The COP_h has an opposite relationship with the gas cooler outlet temperature, which changes in the range of 4.78 to 1.99.

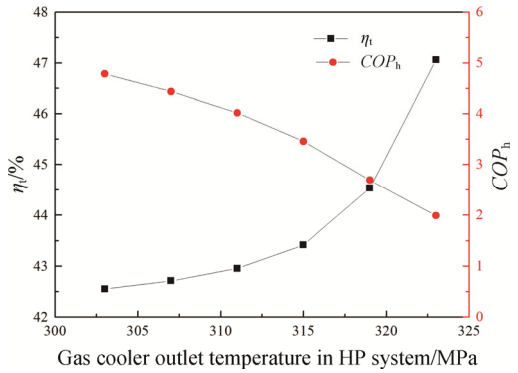

Fig. 10 Total efficiency and COP_h under different gas cooler outlet temperature of HP system

According to the *T-s* diagram, when the gas cooler outlet temperature increases, the heating capacity and power consumption of the compressor correspondingly rise. The increasing rate of heating capacity is less than that of power consumption of the compressor, leading to the decrease of COP_h. Moreover, the increase in heating capacity is greater than that in net power output. Therefore, the thermal efficiency gradually increases according to Eq. (30).

The net power output of the combined system is shown in Fig. 11(a). Generally, the net power output gradually decreases with the gas cooler outlet temperature. The higher the exhaust temperature is, the more obvious the variation of net power output is. When the gas cooler outlet temperature of the HP system is higher than 313 K, the net power output is negative, and the shaft power output of the expander in the ORC is not enough to drive the compressor and the generator at the same time, so the system performance under this condition is poor.

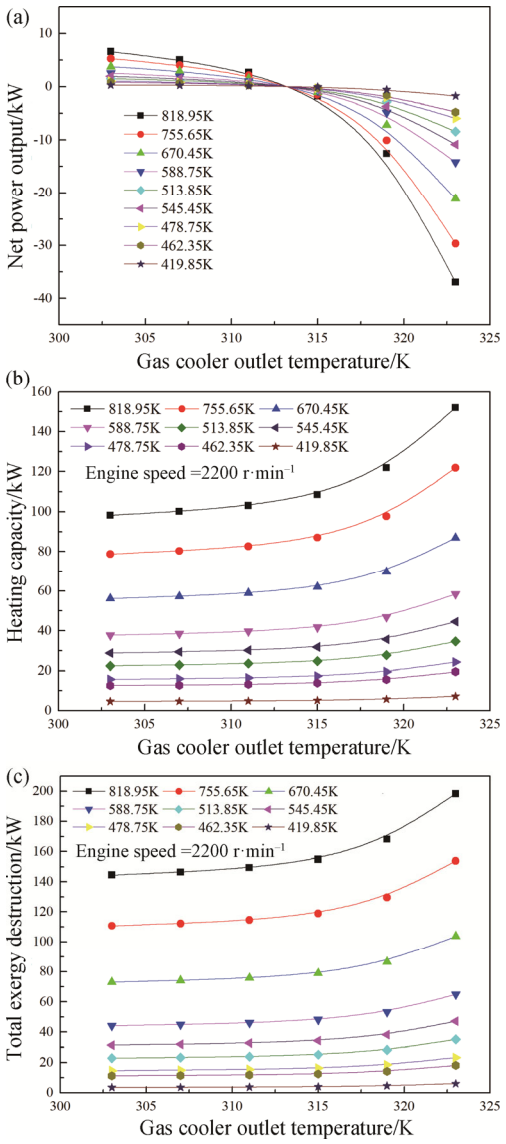

Fig. 11 Net power output, heating capacity and total exergy destruction with gas cooler outlet temperature of HP system

Therefore, the best gas cooler outlet temperature is less than 313 K.

Fig. 11(b) and Fig. 11(c) show the variation of heating capacity and total exergy destruction under different gas cooler outlet temperature. The variation of heating capacity is similar to that of total exergy destruction and they gradually rise with increasing gas cooler outlet temperature. As shown in Fig. 11(c), the total exergy destruction of combined system increases from 144.47 to 198.28 kW with the gas cooler outlet temperature. In addition, the heating capacity and total exergy destruction are progressively sensitive to the gas cooler outlet temperature.

According to Fig. 12, it can be concluded that the variation of evaporation temperature has a significant impact on the performance of the combined system about the total efficiency and COP_h. When the evaporation temperature rises from 273 K to 287 K, the total efficiency decreases from 43.67% to 42.70% and COP_h changes in the range of 3.23 to 4.45. Similarly, the heating capacity and power consumption of the compressor correspondingly decrease with the evaporation temperature, and the decrease in heating capacity is weaker than the decrease in power consumption of the compressor. Therefore, COP_h gradually increases.

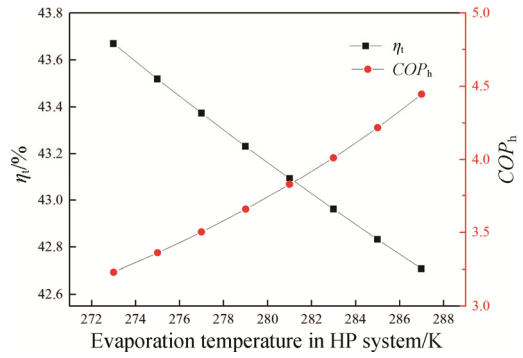

Fig. 12 Total efficiency and COP_h with evaporation temperature of HP system

As indicated in Fig. 13(a), the net power output increases with the evaporation temperature. The net power output is higher than 0 when the evaporation temperature is higher than 281 K. Therefore, the optimum evaporation temperature is higher than 281 K. And the maximum net power output of 3.50 kW can be obtained when the evaporation temperature is 287 K.

Fig. 13(b) and Fig. 13(c) show the same trend with the evaporation temperature. The maximum heating capacity of the HP system decreases from 114.47 to 101.98 kW with increasing the evaporation temperature. The maximum total exergy destruction of combined system decreases from 160.76 kW to 148.27 kW with increasing the evaporation temperature from 273 K to 287 K. Meanwhile, the total exergy destruction goes up with the exhaust temperature and engine speed, and the higher engine speed and exhaust temperature are, the higher total exergy destruction is.

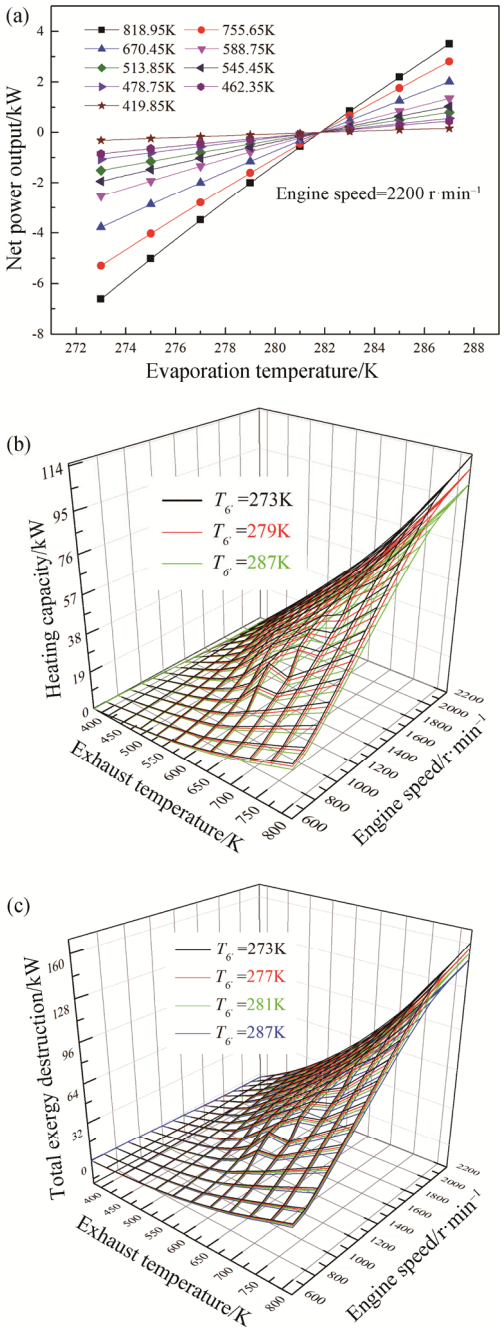

Fig. 13 Net power output, heating capacity and total exergy destruction with evaporation temperature of HP system

5. Conclusions

This paper investigates the performance characteristics of an ORC-HP combined system. The findings indicate that:

(1) Low condensation temperature is conducive to the performance of the combined system, and condensation temperature has a slight influence on the total exergy destruction. There exists a suitable range of evaporation temperature, gas cooler outlet pressure and gas cooler outlet temperature to achieve excellent performance for the combined system. The optimum evaporation temperature is more than 281 K and the optimum gas cooler outlet temperature is less than 313 K.

(2) The exergy destruction of evaporator and condenser decreases with evaporation pressure, and most of the exergy destruction is in evaporator and condenser. It varies rapidly with the exhaust temperature and engine speed. The total exergy destruction decreases from 161.90 to 151.56 kW. The heating capacity and total exergy destruction are sensitive to the change of gas cooler outlet temperature.

(3) The total efficiency shows a first rapidly decreasing and then slowly increasing trend with gas cooler outlet pressure, whereas the COP_h shows an opposite trend with gas cooler outlet pressure, namely there exists an optimal gas cooler outlet pressure that achieves the maximum COP_h. The maximum COP_h of 4.78 can be achieved.

Acknowledgements

This study is financially supported by National Natural Science Foundation of China (Grant No. 51776005, Grant No. 51376011) and National Key R&D Program of China (Grant No. 2016YFE0124900).

References

[1] Dolz V., Novella R., García A., Sánchez J., HD Diesel engine equipped with a bottoming Rankine cycle as a waste heat recovery system. Part 1: Study and analysis of the waste heat energy. Applied Thermal Engineering, 2012, 36: 269–278.

[2] Hou X.C., Zhang H.G., Xu Y.H., Yu F., Zhao T.L., Tian Y.M., Yang Y.X., Zhao R., External load resistance effect on the free piston expander-linear generator for organic Rankine cycle waste heat recovery system. Applied Energy, 2018, 212: 1252–1261.

[3] Hou X.C., Zhang H.G., Yu F., Liu H.D., Yang F.B., Xu Y.H., Tian Y.M., Li G.S., Free piston expander-linear generator used for organic Rankine cycle waste heat recovery system. Applied Energy, 2017, 208: 1297–1307.

[4] Shu G.Q., Liu P., Tian H., Wang X., Jing D.Z., Operational profile based thermal-economic analysis on an organic Rankine cycle using for harvesting marine engine's exhaust waste heat. Energy Conversion and Management, 2017, 146: 107–123.

[5] Singh D.V., Pedersen E., A review of waste heat recovery technologies for maritime applications. Energy Conversion and Management, 2016, 111: 315–328.

[6] Song S.S., Zhang H.G., Zhao R., Meng F.X., Liu H.D., Wang J.F., Yao B.F., Simulation and performance analysis of organic Rankine systems for stationary compressed natural gas engine. Energies, 2017, 10: 544–566.

[7] Yang F.B., Dong X.R., Zhang H.G., Wang Z., Yang K., Zhang J., Wang E.H., Liu H., Zhao G.Y., Performance analysis of waste heat recovery with a dual loop organic Rankine cycle (ORC) system for diesel engine under various operating conditions. Energy Conversion and Management, 2014, 80: 243–255.

[8] Yang F.B., Zhang H.G., Bei C., Song S.S., Wang E.H., Parametric optimization and performance analysis of ORC (organic Rankine cycle) for diesel engine waste heat recovery with a fin-and-tube evaporator. Energy, 2015, 91: 128–141.

[9] Zhao M., Wei M.S., Song P.P., Liu Z., Tian G.H., Performance evaluation of a diesel engine integrated with ORC system. Applied Thermal Engineering, 2017, 115: 221–228.

[10] Yu G.P., Shu G.Q., Tian H., Wei H.Q., Liu L.N., Simulation and thermodynamic analysis of a bottoming organic Rankine cycle (ORC) of diesel engine (DE). Energy, 2013, 51: 281–290.

[11] Song J., Song Y., Gu C.W., Thermodynamic analysis and performance optimization of an organic Rankine cycle (ORC) waste heat recovery system for marine diesel engines. Energy, 2015, 82: 976–985.

[12] Song J., Gu C.W., Parametric analysis of a dual loop organic Rankine cycle (ORC) system for engine waste heat recovery. Energy Conversion and Management, 2015, 105: 995–1005.

[13] Saleh B., Koglbauer G., Wendland M., Fischer J., Working fluids for low-temperature organic Rankine cycles. Energy, 2007, 32: 1210–1221.

[14] Liu B.T., Chien K.H., Wang C.C., Effect of working fluids on organic Rankine cycle for waste heat recovery. Energy, 2004, 29: 1207–1217.

[15] Tian H., Shu G.Q., Wei H.Q., Liang X.Y., Liu L.N., Fluids and parameters optimization for the organic Rankine cycles (ORCs) used inexhaust heat recovery of internal combustion engine (ICE). Energy, 2012, 47: 125–136.

[16] Wang E.H., Zhang H.G., Fan B.Y., Ouyang M.G., Zhao Y., Mu Q.H., Study of working fluid selection of organic Rankine cycle (ORC) for engine waste heat recovery. Energy, 2011, 36: 3406–3418.

[17] Feng Y.Q., Hung T.C., He Y.L., Wang Q., Wang S., Li B.X., Lin J.R., Zhang W.P., Operation characteristic and performance comparison of organic Rankine cycle (ORC)

for low-grade waste heat using R245fa, R123 and their mixtures. Energy Conversion and Management, 2017, 144: 153–163.

[18] Demierre J., Rubino A., Schiffmann J., Modeling and experimental investigation of an oil-free microcompressor-turbine unit for an organic Rankine cycle driven heat pump. Journal of Engineering for Gas Turbines and Power, 2015, 137: 032602-1–032602-10.

[19] Mago P.J., Fumo N., Chamra L.M., Performance analysis of CCHP and CHP systems operating following the thermal and electric load. International Journal of Energy Research, 2009, 33: 852–864.

[20] Li X.J., Zhang X.R., Preliminary investigation of a transcritical CO_2 heat pump driven by a solar-powered CO_2 Rankine cycle. International Journal of Energy Research, 2013, 37: 1361–1371.

[21] Fang F., Wei L., Liu J.Z., Zhang J.H., Hou G.L., Complementary configuration and operation of a CCHP-ORC system. Energy, 2012, 46: 211–220.

[22] Agrawal N., Bhattacharyya S., Experimental investigations on adiabatic capillary tube in a transcritical CO_2 heat pump system for simultaneous water cooling and heating. International Journal of Refrigeration, 2011, 34: 476–483.

[23] Antonijevic D., Heckt R., Heat pump supplemental heating system for motor vehicles. Proceedings of the Institution of Mechanical Engineers Part D Journal of Automobile Engineering, 2004, 218: 1111–1115.

[24] Wang Z.H., Wei M.S., Guo C., Zhao M., Enhance the heating performance of an electric vehicle AC/HP System under low temperature. Energy Procedia, 2017, 105: 2384–2389.

[25] Wang Z.H., Wei M.S., Peng F.Z., Liu H.B., Guo C., Tian G.H., Experimental evaluation of an integrated electric vehicle AC/HP system operating with R134a and R407C. Applied Thermal Engineering, 2016, 100: 1179–1188.

[26] Qin F., Zhang G.Y., Xue Q.F., Zou H.M., Tian C.Q., Experimental investigation and theoretical analysis of heat pump systems with two different injection portholes compressors for electric vehicles. Applied Energy, 2017, 185: 2085–2093.

[27] Qin F., Xue Q.F., Velez G.M.A., Zhang G.Y., Zou H.M., Tian C.Q., Experimental investigation on heating performance of heat pump for electric vehicles at −20°C ambient temperature. Energy Conversion and Management, 2015, 102: 39–49.

[28] Cao Y., Gao Y.K., Zheng Y., Dai Y.P., Optimum design and thermodynamic analysis of a gas turbine and ORC combined cycle with recuperators. Energy Conversion and Management, 2016, 116: 32–41.

[29] Feng Y.Q., Hung T.C., Zhang Y.N., Li B.X., Yang J.F., Shi Y., Performance comparison of low-grade ORCs (organic Rankine cycles) using R245fa, pentane and their mixtures based on the thermoeconomic multi-objective optimization and decision makings. Energy, 2015, 93: 2018–2029.

[30] Chen H., Performance evaluation and design of heat pump air conditioning for electric bus. Zhongyuan University of Technology, Zhengzhou, China, 2016.

[31] Liao S.M., Zhao T.S., Jakobsen A., A correlation of optimal heat rejection pressures in transcritical carbon dioxide cycles. Applied Thermal Engineering, 2000, 20: 831–841.

[32] Bahadori A., Estimation of combustion flue gas acid dew point during heat recovery and efficiency gain. Applied Thermal Engineering, 2011, 31: 1457–1462.

[33] Sadeghi M., Nemati A., Ghavimi A., Yari M., Thermodynamic analysis and multi-objective optimization of various ORC (organic Rankine cycle) configurations using zeotropic mixtures. Energy, 2016, 109: 791–802.